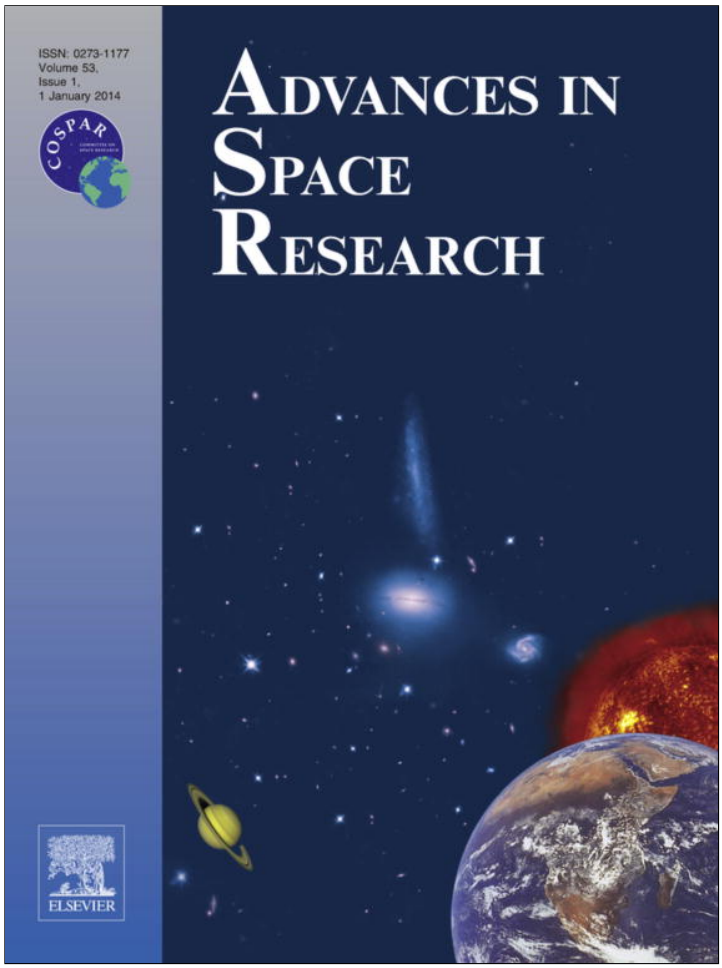

Available online at www.sciencedirect.com

ScienceDirect

Advances in Space Research 53 (2014) 110–118

ADVANCES IN SPACE RESEARCH (a COSPAR publication)

www.elsevier.com/locate/asr

Active space debris charging for contactless electrostatic disposal maneuvers

Hanspeter Schaub [a,*,1], Zoltán Sternovsky [b]

[a] Aerospace Engineering Sciences Department, University of Colorado, Boulder, CO 80309, United States

[b] Laboratory for Atmospheric and Space Physics, Aerospace Engineering Sciences Department, University of Colorado, Boulder, CO 80303, United States

Received 21 May 2013; received in revised form 2 October 2013; accepted 7 October 2013
Available online 14 October 2013

Abstract

The remote charging of a passive object using an electron beam enables touchless re-orbiting of large space debris from geosynchronous orbit (GEO) using electrostatic forces. The advantage of this method is that it can operate with a separation distance of multiple craft radii, thus reducing the risk of collision. The charging of the tug–debris system to high potentials is achieved by active charge transfer using a directed electron beam. Optimal potential distributions using isolated- and coupled-sphere models are discussed. A simple charging model takes into account the primary electron beam current, ultra-violet radiation induced photoelectron emission, collection of plasma particles, secondary electron emission and the recapture of emitted particles. The results show that through active charging in a GEO space environment high potentials can be both achieved and maintained with about a 75% transfer efficiency. Further, the maximum electrostatic tractor force is shown to be insensitive to beam current levels. This latter later result is important when considering debris with unknown properties.

Keywords: Space debris; Electrostatic tractor; Electron beam

1. Introduction

The threat of space debris on satellite operations has increased to the point where avoiding creating debris is no longer sufficient (Johnson, 2010). The tipping point has been reached where the low-Earth orbit space debris population will continue to increase even if no additional satellites are launched, due to debris–debris collisions (Liou, 2011). While having less debris than the Low Earth Orbit (LEO) regions, the Geostationary Earth Orbit (GEO) region is a very narrow zone with a growing number of large, defunct Earth sensing and communication satellites, as well as spent rocket bodies. Of the over 1200 large GEO object tracked, less than 400 are controlled, functioning satellites (Jehn et al., 2005). The GEO satellites are high-value spacecraft, and the GEO space debris concern is a growing concern with operators and associate insurance agencies (Chrystal et al., 2011). International guidelines specify that GEO spacecraft must move to a disposal orbit at their end of life. However, this is not done by all operators, or technical failures prevent this final step. Thus, active debris removal at GEO is a critical capability to avoid frequent debris avoidance maneuvers (Anderson and Schaub, 2013).

Active debris removal (ADR) remains a challenging discipline with no solutions operating in space (Richards et al., 2005). Envisioned concepts range from robotic docking (Smith et al., 2004; Bosse et al., 2004), electrodynamics tethers for LEO applications (Pearson et al., 2003), electric sails(Janhunen et al., 2013), as well as space debris pushers using contactless directed ion exhaust plumes (Bombardelli and Pelaez, 2011; Bombardelli et al., 2011; Kitamura, 2010). Schaub and Moorer (2010) discuss a novel, patented

* Corresponding author. Tel.: +1 3034922767.
E-mail addresses: hanspeter.schaub@colorado.edu (H. Schaub), zoltan.sternovsky@lasp.colorado.edu (Z. Sternovsky).
[1] H. Joseph Smead Fellow.

0273-1177/$36.00 © 2013 COSPAR. Published by Elsevier Ltd. All rights reserved.
http://dx.doi.org/10.1016/j.asr.2013.10.003

approach to moving large, tumbling GEO debris to disposal orbits 250–300 km above the geosynchronous zone as illustrated in Fig. 1. Here the tug employs continuous electron emission to raise its own potential to a positive value of 10s of kilo-volts, while the electron emission is directed at the space debris object to yield a negative potential. Simultaneously low-thrust inertial thrusters are employed on the tug to raise the two-vehicle system altitude (Moorer and Schaub, 2011b,a). Thrusters must be selected whose exhaust plume does not impinge on the charged neighboring space object. Neutral gas thrusters could be used, as the Δv requirement to move a debris object to the disposal orbit is only about 11 m/s. The resulting attractive inter-vehicle force is referred to as the electrostatic tractor (ET) and will reach magnitudes of several milli-Newtons assuming a separation distance of 15–25 m. Even large multi-ton debris objects can be moved or reorbited to a disposal orbit in 2–4 months (Schaub and Jasper, 2011). The pulling configuration with attractive electrostatic forces is preferred due to (a) increased forces for a given potential, (b) passively stable relative orientation, as well as (c) superior failure modes having the tug pull away safely if the ET fails (Schaub and Jasper, 2013).

The focus of this paper is the charge transfer process itself for this ET concept. Established fundamental plasma physics and charging models are applied to the ET concept to evaluate ideal potential distributions between the tug and debris, as well as approximated expected charge transfer efficiencies. To obtain analytical approximations of the expected ET force, the spacecraft are assumed to be spherical. Jasper and Schaub (2012) discuss why this is a reasonable assumption, even with large GEO communication satellite shapes, if the separations are 2–3 craft radii.

Active charge control for space-based actuation is first discussed by Cover et al. (1966), were the GEO region is identified as ideal for active charging applications where kilo-volts of potential can be achieved using as little as watt-levels of electrical power. Cover discusses using these forces for electrostatic membrane inflation. King et al. (2003) discusses active charge control to directly control relative motion of spacecraft having identified that the naturally occurring space weather related charging observed on the SCATHA (Mullen et al., 1986) and ATS missions could lead to significant disturbance forces on nearby space objects. This has led to extensive research studying charged relative motion dynamics for cluster and formation flying (Natarajan and Schaub, 2008; Wang and Schaub, 2011). Recently, the use of hybrid actuation (employing both electrostatic forces and inertial thrusters) to control the relative motion while performing inertial orbit corrections is discussed by Hogan and Schaub (2013). This work identifies the importance of ET effectiveness bounds in the relative motion stability analysis. The ET concept is also discussed by Murdoch et al. (2008) for asteroid deflection applications. This work illustrates that with large space object potentials relative to the plasma energies, the Debye length related shielding of electrical charges is reduced. For the GEO debris application the average minimal Debye lengths are on the order of 180–200 m (Denton et al., 2005), making Debye shielding concerns minimal for the ET operation.

The ET concept is also of interest for on-orbit servicing of satellites to enable novel relative motion control with the to-be-serviced satellite, including touchless repositioning as discussed by Hogan and Schaub (2012). The servicing missions considered may include refueling, part replacement or repair and forced orbit change. There are a number of envisioned concepts, including using (a) robotic arms for docking and deployment of de-orbiting devices (Bosse et al., 2004; Castronuovo, 2011; Xu et al., 2011), or (b) non-robotic capture with nets, tethers or inflatable devices (Pearson et al., 2003; Kawamoto et al., 2006).

The prior Coulomb actuation studies do not consider the electron charge transfer process between two space objects. The active charge emission is performed on each space object individually, and is assumed to not impact the charging of a neighboring object. This paper performs an analytical study of how well the ET concept will operate taking into account the diverse spacecraft charging effects due the plasma space environment, photo-electron current, secondary electron emission, as well as the charge imparted by the space tug. The charge transport onto space particles is studied by the dusty plasma community (Sternovsky et al., 2001; Žilavý et al., 1998). Plasma analysis tools are employed to study the ET effectiveness for GEO debris actuation. Of interest are what ideal tug and debris potentials yield the best ET magnitude given the limited charge emission energies, the effectiveness of the charge transfer process for a range of tug potentials, as well as the sensitivity of the ET performance on tug potential uncertainties.

The article is organized as follows. In Section 2 the main forces acting on the tug–debris system are discussed. Of

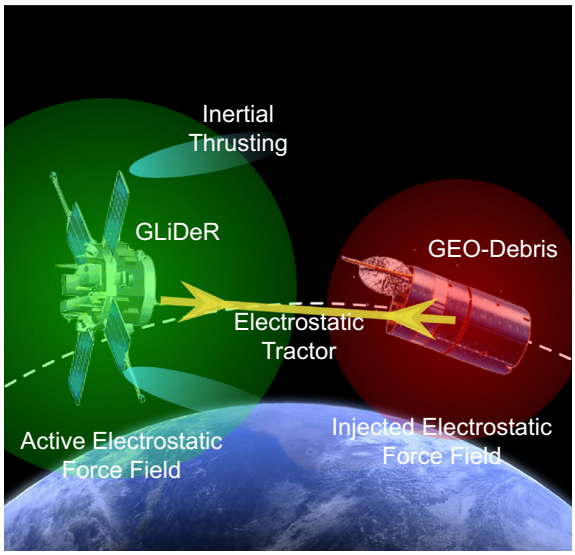

Fig. 1. Illustration of the geosynchronous large debris reorbiter (GLiDeR^{TM}) concept.

interest is if ET forces in the milli-Newton range are feasible at a distance of 10–20 m. This force magnitude has been shown to yield multi-ton debris reorbiting times of 2–3 month (Schaub and Jasper, 2011). Further, benefits of using electron rather than ion emission are investigated. In Section 3 the charging currents are presented, which include primary processes (photoelectron emission, collection of electrons and ions from the plasma environment and the active charge transfer) as well as secondary processes (secondary electron emission due to impinging primary electrons, collection of particles emitted by one craft by the other). Section 4 discusses the plasma conditions of the GEO environment. Numerical solutions to the charging problem are presented in Section 5.

2. Electrostatic forces between tug and debris

2.1. Force models

In order to gain insight into the touchless active charging effectiveness and sensitivity, a reduced-order analytical form is employed which captures the primary current contributors. The first simplifying assumption is that both the tug and the debris are conductive spheres. Current GEO spacecraft design requires all outer surfaces to be conductively connected, thus avoiding differential charging. While GEO spacecraft are not spherical, this is a good assumption if the separation distance is large enough. Jasper and Schaub (2012) demonstrates how such spherical approximations are reasonable for general spacecraft shapes if the separation distances are more than 2–3 spacecraft dimensions. The difference in the electrostatic force between a cylinder and a sphere is about 5–25% if a sphere–sphere model with proper effective radii is used.

The two main forces acting between the objects are the attractive Coulomb force and the momentum transferred from the tug to the debris by the charging beam, which represents a repulsive force. The Coulomb force acting between point charges in the plasma environment at a separation distance r is written in a simple form:

$$F_C = k_c \frac{Q_T Q_D}{r^2} e^{-r/\lambda_D}\left(1+\frac{r}{\lambda_D}\right) \tag{1}$$

where Q_T and Q_D are the charges on the tug and the debris, respectively. The Boltzman constant is $k_c = 1/4\pi\epsilon_0$, where ϵ_0 is the permittivity of vacuum. The distance between the object center of masses is r, and λ_D is the *effective Debye length* of the ambient plasma (Murdoch et al., 2008). Because the tug–debris separation distances considered are on the order of dozens of meters, and the nominal GEO Debye length is around 200 m (Denton et al., 2005), it is a good assumption to ignore the plasma influence on the electrostatic tractor force calculation. As a result the exponential term in Eq. (1) is dropped for all future calculations. The justification for doing so is that λ_D is large for common conditions for GEO plasma (see Section 4) and that the Debye shielding effect is reduced for objects charged to much higher potentials than the temperature of the plasma particles (Stiles et al., 2012).

The force model in Eq. (1) is also valid if two charged spheres are considered instead of two point charges. If the separation distance r is larger than 15–20 craft radii (Schaub and Jasper, 2013), the self-capacitance of each sphere can be used to relate stored charge Q to the surface voltage ϕ. The following investigation will use the simpler isolated sphere model first to gain insight into ideal potential distribution for the maximum electrostatic tractor force F_C. Next, a more general result with a coupled capacitance model is considered. Using this isolated sphere model, the charge and the potential on the objects are related through

$$Q_T = \frac{R_T}{k_c}\phi_T \tag{2a}$$

$$Q_D = \frac{R_D}{k_c}\phi_D \tag{2b}$$

where ϕ_T and ϕ_D are the potentials with respect to the undisturbed space potential of the tug and debris, respectively. The parameters R_T and R_D are effective tug and debris radii. With the effective sphere model (Jasper and Schaub, 2012), the E-field of a general shape is approximated with a single sphere whose size is given by the effective radius. Such models match the true E-fields well at a distance, but yield modeling errors of 10–20% if within 2–3 mean craft radii. With the effective spacecraft radius $R \ll \lambda_D$ condition satisfied, the plasma impact on the capacitance can be neglected. For shorter Debye lengths, the plasma can increase the objects capacitance (Peck, 2005; Stiles et al., 2012). The attractive force can be enlarged by increasing the potentials on the crafts, increasing the capacitance (size) of the tug, or reducing the separation distance. The latter would be the obvious choice, except that collisions with potentially devastating outcomes have to be avoided. Schaub and Jasper (2013) show that a separation distance on the order of 15–20 m, considering for example a debris radius of 2–3 m, provides both a sufficient attractive force for GEO debris reorbiting at craft potentials on the order of 10s of kilo-volts. Schaub and Jasper (2013) show that the effective radii for defunct GEO satellites can range from 1 to 6 m. A common 2-ton satellite has an effective radius of about 2–3 m. However, this prior work did not consider the constraints of achieving potentials using an electron gun, nor does it discuss the effectiveness and sensitivity of this charge transfer process in a plasma environment.

Next, assume a scenario with two nearby conducting spheres as illustrated in Fig. 2. The potential ϕ_T on the tug is computed as the sum of the self-capacitance relationship and the potential due to the debris charge Q_D as (Sliško and Brito-Orta, 1998):

$$\begin{bmatrix}\phi_T\\ \phi_D\end{bmatrix} = k_c \begin{bmatrix}\frac{1}{R_T} & \frac{1}{r}\\ \frac{1}{r} & \frac{1}{R_D}\end{bmatrix}\begin{bmatrix}Q_T\\ Q_D\end{bmatrix} \tag{3}$$

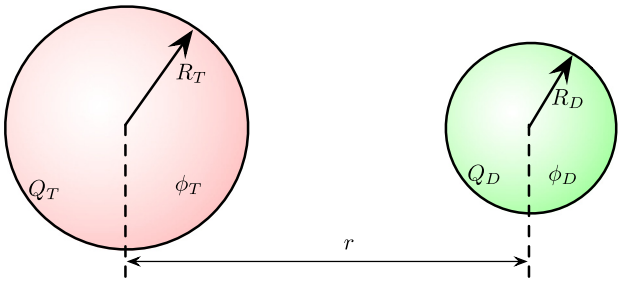

Fig. 2. Illustration of two close proximity charged spheres.

Even with spheres held at fixed potentials, the charge distribution can be non-homogenous (Soules, 1990). However, this induced charge effect is negligible if the separation distance is more than 3 craft radii as is assumed in this study. Inverting Eq. (3) for the charges yields:

$$\begin{bmatrix} Q_T \\ Q_D \end{bmatrix} = \underbrace{\frac{r}{k_c(r^2 - R_T R_D)} \begin{bmatrix} R_T r & -R_T R_D \\ -R_T R_D & R_D r \end{bmatrix}}_{[C(r)]} \begin{bmatrix} \phi_T \\ \phi_D \end{bmatrix} \tag{4}$$

The 2×2 matrix $[C(r)]$ is the capacitance matrix for this two-sphere system which is a function of the separation distance. The presence of a charged neighboring object impacts the capacitance of the debris and tug objects. This increases the attractive force in an opposite potential configuration, and will decrease the repulsive force in an equal potential configuration (Schaub and Jasper, 2013).

2.2. Optimal tug and debris potentials

Next, the optimal potential assignment for the tug and debris objects is considered. Charged particles can be actively transferred from the tug to the debris by electron or ion guns. Considering vacuum conditions, the potential difference U is then driven between the tug and debris,

$$U = \phi_T - \phi_D \tag{5}$$

by the active charge transfer. Considering an ambient plasma environment, the potential difference U has to be smaller than the gun energy due to the discharging currents from the ambient plasma and UV photoemission.

$$U \leqslant E_{EB}/q = U_{\max} \tag{6}$$

where q is the elementary charge and E_{EB} is the energy of the accelerated beam particles measured in eV. Thus, assuming a vacuum condition for now, the potential difference is set equal to the beam potential with $U = U_{\max}$.

Using the potential difference constraint $\phi_T = U + \phi_D$, and assuming an isolated sphere model in Eq. (2) to begin with, the electrostatic tractor force is given by:

$$F_c = \frac{R_T R_D}{k_c r^2} \phi_D (U + \phi_D) \tag{7}$$

To determine the extremum of this tractor force, the first order sensitivity of F_c with respect to ϕ_D is set to zero:

$$\frac{\partial F_c}{\partial \phi_D} = \frac{R_T R_D}{k_c r^2}(U + 2\phi_D) = 0 \tag{8}$$

For a given potential difference U, the strongest electrostatic tractor force occurs when the potential magnitude is equally shared between the tug and the debris:

$$\phi_T = \frac{U}{2} \quad \phi_D = -\frac{U}{2} \tag{9}$$

This elegant result is based on the assumption that the isolated sphere model is correct for the capacitance evaluation. In this case the extremum of the electrostatic tractor force is

$$F_{c,\max} = -\frac{R_T R_D}{k_c r^2} \frac{U^2}{4} \tag{10}$$

Next, the position dependent capacitance in Eq. (4) is considered. Applying the voltage difference constraint $\phi_T = U + \phi_D$, the electrostatic tractor force is now expressed as:

$$F_c = -\frac{R_T R_D}{k_c (r^2 - R_T R_D)^2}(R_D \phi_D - r(U + \phi_D)) \cdot (r\phi_D - R_T(U + \phi_D)) \tag{11}$$

To find the debris potential ϕ_D that yields an extremum of the electrostatic tractor, the first order sensitivity is set equal to zero again:

$$\frac{\partial F_c}{\partial \phi_D} = \frac{R_T R_D}{k_c (r^2 - R_T R_D)^2} \big(U(r^2 - 2rR_T + R_T R_D) + 2\phi_D (r - R_D)(r - R_T)\big) = 0 \tag{12}$$

Solving Eq. (12) for the debris potential ϕ_D, and using the potential constraint in Eq. (5), yields the optimal tug and debris potentials for the strongest electrostatic tractor force:

$$\phi_T = \frac{U}{2} \frac{(r^2 - 2rR_D + R_T R_D)}{(r - R_T)(r - R_D)} \tag{13a}$$

$$\phi_D = -\frac{U}{2} \frac{(r^2 - 2rR_T + R_T R_D)}{(r - R_T)(r - R_D)} \tag{13b}$$

Note that if the effective radii are equal with $R_T = R_D$, then the equal potential split condition in Eq. (9) is regained. Thus, the isolated sphere model is still a good approximation to determine the optimal tug and debris potential distribution if the respective effective radii are about the same.

To visualize how the tug–debris potentials deviate from this equal-split condition if the higher fidelity position dependent capacitance model in Eq. (4) is used, assume that $R_D = \gamma R_T$ with $\gamma > 0$. If $\gamma = 1$ then the tug and debris are modeled as having the same effective size. Fig. 3 illustrates the resulting tug and debris potential surfaces assuming $U = 20$ kV. The separation distance is 15 m and the tug has an effective radius of 3 m. If the craft radii are equal, the optimal potentials are equal regardless of separation distance. If the debris is larger than the tug ($\gamma > 1$) the optimal tug potential is larger then the debris potential, and vice-verse if the debris is smaller than the tug. Also, as the separation distance increases, the difference in

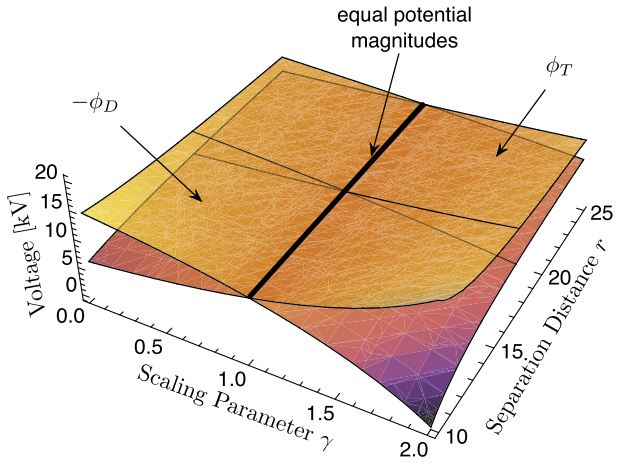

Fig. 3. Optimal potential surfaces assuming $U = 20$ kV and $R_T = 3$ m.

optimal potential magnitudes becomes smaller, near negligible. For very close approaches with 10 m and $\gamma = 2$, the objects are within 1 m of touching each other. In such a near-docking scenario the optimal potentials can deviate significantly from the earlier equal-potential condition. However, if such docking scenarios are considered, further analysis is required to include the induced charging effects which become significant if the vehicle separation is less than 2–3 craft radii.

Using the optimal potential distribution in Eq. (13), the strongest electrostatic tractor force is expressed as:

$$F_{c,\max} = -\frac{R_T R_D}{k_c(r - R_T)(r - R_D)} \frac{U^2}{4} \tag{14}$$

As has been discussed in Schaub and Jasper (2013), considering the coupled capacitance model in Eq. (4) leads to an increased electrostatic tractor performance for the pulling (attractive force) configuration. Fig. 4 compares the electrostatic tractor force levels for a scenario where $U = 20$ kV, the separation distance is $r = 15$ m, and the tug has a radius of 3 m. The optimal isolated sphere ET force from Eq. (10) significantly under-predicts the resulting attraction in comparison to the higher fidelity performance model in Eq. (14). If the equal potential condition is used with the coupled capacitance model in Eq. (4), the decrease in the resulting attraction is minimal for this debris tugging scenario. This illustrates that the equal potential condition is a good starting point for the electrostatic debris tugging application unless the debris is much larger than the tug, or very close separation distances are considered.

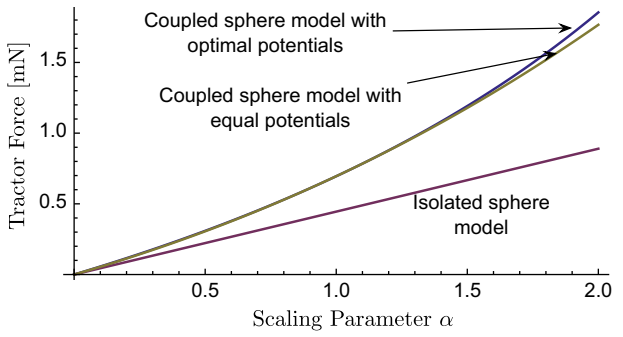

Fig. 4. Electrostatic force comparison assuming $U = 20$ kV, $R_T = 3$ m and $r = 15$ m.

2.3. Repulsion due to charge transfer

The current transferred by charged particles represents a repulsive force between the tug and debris. This force is from (a) the thrust from the particles leaving the tug, and (b) the thrust from the particles impacting the debris. The thrust force is calculated as the change of momentum over a unit time. Under the assumptions that the beam consists of singly charged particles, all particles leaving the tug impact on the debris and are absorbed, and equilibrium charge conditions ($|\phi_T| < E_{EB}/2$) are present, the magnitude of this force is approximated as

$$F_R = 2\frac{I_{tr}}{q} m_b v_\infty \tag{15}$$

where I_{tr} is the current of transmitted beam, q is the elementary charge, and

$$v_\infty = \sqrt{\frac{2q(E_{EB} - \phi_T)}{m_b}} \tag{16}$$

is the velocity of the beam particles at infinity. The parameter m_b is the mass of the beam particles, which are either electrons or ions. For electrostatic pulling to work, the Coulomb interaction has to be stronger than the repulsive thrust, i.e. $F_C > F_R$. Fig. 5 shows the comparison of the two forces as a function of separation distance for typical charging current conditions. The calculations are for $I_{tr} = 0.8$ mA, $E_{EB} = 60$ keV, $\phi_T = 28$ kV, Ar^+ ions and electrons. Using standard commercial technology is feasible to emit currents in the 1–10 mA range without space charge playing an effect. The tug and debris are spheres

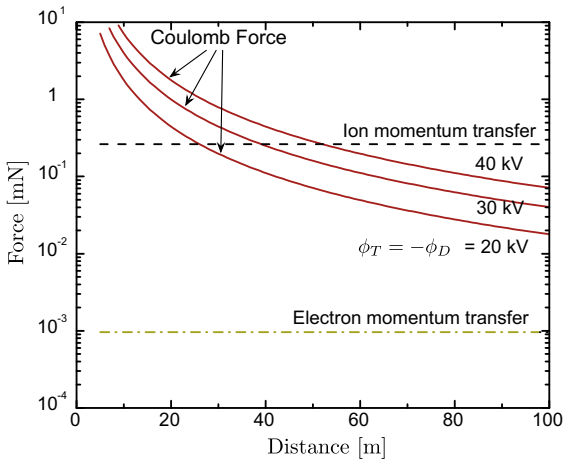

Fig. 5. The comparison of the attractive Coulomb force (without Debye shielding) to the repulsive force of electrons or ions from the active charge transfer.

of $R = 2$ m radius. The values of these parameters are justified in Section 5. The Coulomb force for potentials 20 kV, 30 kV and 40 kV are compared using the isolated sphere models. The repulsive force is a factor $\sqrt{m_i/m_e}$ larger for ions with mass m_i than for electrons of mass m_e. The following observations can be made: for crafts with 2 m average radius charged to tens of kV potential, the Coulomb force is in the mN range for separation distance at around 20 m. The repulsive force from an ion charging beam is close to the mN level and is independent of the separation distance. Active charging by an electron beam, on the other hand, transfers little momentum and its repulsive effect is negligible. Charging by an electron beam is thus the preferred option, which is incidentally also easier to implement and reduces the requirement for fuel mass. As a result, the tug will be positively charged and the debris negatively charged. The thrust forces from all other collected or emitted particles are assumed to be isotropic with a zero net effect.

3. Craft charging model

Besides the active charge transfer from the tug to the debris, there are a number of primary charging processes from the space environment and also secondary processes that will affect the attainable potentials. This section presents the analytical formulas for the charging currents. The equilibrium potential of the tug–debris system is achieved by the current balance; i.e. when the net current to each object is zero. The tug is charging positively because of the active emission of electrons, while the debris will acquire negative charge. For generality it is also assumed that the tug is equipped with an auxiliary ion gun that can purge unwanted charge, if necessary.

The photoelectron current from solar UV radiation is written in a form (Lai, 2011):

$$I_{ph}(\phi) = j_{ph,0} A_\perp e^{-\phi/T_{ph}} \quad \phi > 0 \tag{17a}$$

$$= j_{ph,0} A_\perp \quad \phi \leqslant 0 \tag{17b}$$

where $j_{ph,0}$ and T_{ph} are the flux and temperature of the emitted photoelectrons, $A_\perp$ is the cross section of the spacecraft exposed to UV. The value of is on the order of 10 $\mu A/m^2$ depending on surface material of the spacecraft and can vary by up to a factor of 8 with solar activity (Sternovsky et al., 2008). The values used in this article are $j_{ph,0} = 20\ \mu A/m^2$ and $T_{ph} \approx 2$ eV.

The collection of plasma electrons from the surrounding plasma is given by (Pfau and Tichy, 2001):

$$I_e(\phi) = -\frac{Aqn_e w_e}{4} e^{\phi/Te} \quad \phi < 0 \tag{18a}$$

$$= -\frac{Aqn_e w_e}{4}\left(1 + \frac{\phi}{T_e}\right) \quad \phi \geqslant 0 \tag{18b}$$

where $A = 4\pi R^2$ is the surface area of the craft and $w_e = \sqrt{8T_e/(\pi m_e)}$ is the thermal velocity of the plasma electrons. The minus sign defines the polarity of this current. The collection of plasma ions is similar in form and in the definition of the variables (Pfau and Tichy, 2001):

$$I_i(\phi) = \frac{Aqn_i w_i}{4} e^{-\phi/T_i} \quad \phi > 0 \tag{19a}$$

$$= \frac{Aqn_i w_i}{4}\left(1 - \frac{\phi}{T_i}\right) \quad \phi \leqslant 0 \tag{19b}$$

The active charge transfer is performed by the means of an electron gun on the tug that is pointed at the debris. Some fraction of the emitted electrons from the gun reach the debris, depending on the charge state of the two crafts and the energy of the electron beam:

$$I_D(\phi_D) = -\alpha I_{T,0} \quad \phi_T - \phi_D < E_{EB} \tag{20a}$$

$$= 0 \quad \phi_T - \phi_D \geqslant E_{EB} \tag{20b}$$

where $I_{T,0}$ is the electron current emitted from the tug and α is the factor of charge transfer efficiency that incorporates the effects from pointing accuracy of the electron beam at the debris and the width of the beam at the location of the debris. Furthermore, α is in general a function of the potentials on the tug and debris and the beam energy. Upon impact on the debris, the primary electrons from the gun will induce the emission of secondary electrons. The secondaries will leave the debris because of its large negative potential and thus represent an additional charging current. We use the approximation by Draine and Salpeter (1979) to describe the current of secondary electron emission from the debris :

$$I_{\mathrm{SEE}}(\phi_D) = 4Y_M I_D(\phi_D)\kappa \quad \phi_D < 0 \tag{21a}$$

$$= 0 \quad \phi_D \geqslant 0 \tag{21b}$$

Here

$$\kappa = \frac{E_{\mathrm{eff}}/E_{\max}}{(1 + E_{\mathrm{eff}}/E_{\max})^2} \tag{22}$$

and

$$E_{\mathrm{eff}} = E_{EB} - \phi_T + \phi_D \tag{23}$$

is the effective energy of the primary electron impacting the surface of the debris. Y_M is the maximum yield of secondary production, defined as the average number of electrons emitted for each impacting electron. $E_{\max}$ is the impact energy at which this maximum occurs. Typical values of Y_M are on the order of one for most metal surfaces but can be much larger for insulators. The values for aluminum, for example, are $E_{\max} = 300$ eV and $Y_m = 1$ for normal incidence. The electron yield, however, increases with impact angle and the average yield from a spherical object is approximately twice as large as from a planar surface at normal incidence.

4. Plasma environment

At geosynchronous orbits the crafts are exposed to a plasma environment that varies with local time and

geomagnetic activity. The magnetospheric plasma consists of electrons, protons and singly-charged oxygen ions. The statistical studies by Denton et al. (2005) provide a convenient summary of electron density and temperature properties under various geomagnetic activity levels for a range of K_p indexes. Extreme plasma conditions related to solar flares do exist, however, these are short lived compared to the time scale of re-orbiting (approximately a few months). The prime interest is thus investigating the craft charging processes for the most common conditions. The best statistical representation of geomagnetic activity conditions is described by $K_p \leqslant 3$, which applies about 80% of the time (Korth et al., 1999). The K_p value is an index of solar activity, with 1 being low, and 5 being a solar storm condition.

In general, the electron densities are highest on the morning side of the magnetosphere (under quiet conditions), and lower in the afternoon sector. The variation is roughly between 0.1 and 1 cm^{-3} and the typical value of $n_e = 1.25\ cm^{-3}$ is used in the calculations below. The electron temperature can vary in the range of 100–2500 eV, but the temperature rises to or above 1000 eV level only in the early morning section. The typical value of $T_e = 900$ eV is used. The ion density and temperatures are set equal to that of the electrons for the charge neutrality requirement. It ought to be noted that with respect to the magnetic field, the temperatures of both the electrons and ions can be divided into parallel and perpendicular components, which can differ by a small amount. This effect however is neglected and it is also assumed that all ions are protons.

The characteristic Debye length of the plasma,

$$\lambda_D = \sqrt{\frac{\epsilon_0 T_{e,j}}{q n_e}} \tag{24}$$

where the temperature is measured in the units of eV, is on the order of hundreds of meters (Denton et al., 2005). It is thus justified to neglect the exponential shielding term in Eq. (1) for the calculation of the electrostatic force.

5. Numerical solutions

Fig. 6 shows the magnitude of the different currents to the debris as a function of its potential. This example is calculated for a case of 1m radius spherical objects, the electron beam energy is $E_{EB} = 20$ kV. The electron gun operates at $I_{T,0} = 120$ μA emission and normal plasma conditions are assumed. The 1 m radius provides a simple test case which falls within the 1–6 m range of observed GEO debris effective radii. The potential established on the tug is calculated from the current balance, $I_e + I_{T,0} = 0$, and results in a potential of $\phi_T = 7.651$ kV. It is assumed that electron beam is well focused and accurately pointed at the debris and thus $\alpha = 1$ from above. The potential established on the debris is also calculated from the current balance and results in $\phi_D = -7.671$ kV. The potential

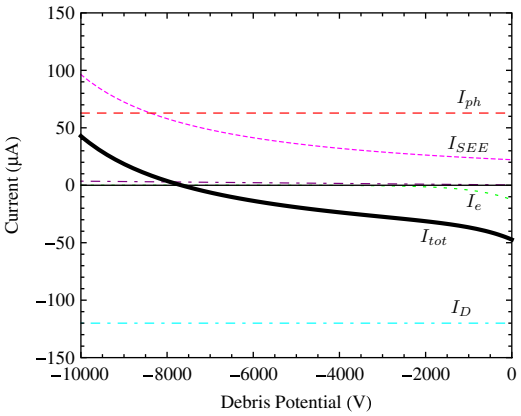

Fig. 6. Current illustration for ranges of debris potentials.

difference reached between the two objects is thus $U = 15.322$ kV. While smaller than the energy of the electron beam by about 25%, this still leaves a considerable potential difference that is suitable for electrostatic tugging of GEO debris to a 300 km higher disposal orbit (Schaub and Jasper, 2013). Note that these results are for the particular scenario shown. If different effective radii or plasma conditions are considered, the results will vary. A full study of the ET performance sensitivity to radii and plasma variations is being investigated in future research.

A parametric study of the tug and debris charging is performed as a function of the magnitude of the active charging current. The results are shown in Fig. 7 and the observations can be summarized as follows. The tug potential (top figure) increases linearly with the emitted current. This is because the only compensating current is plasma electron collection from the environment, which is also a linear function of the tug potential. The debris potential (second from top) is a non-linear and non-monotonic function of the transferred current. At the beginning, the debris

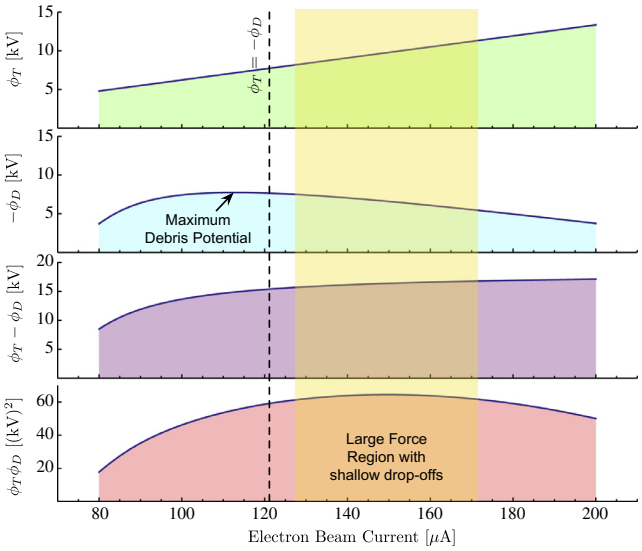

Fig. 7. Potentials for a range of electron beam currents.

potential increases because of the increasing electron beam charging current. The subsequent decrease is due to the fixed energy (20 kV) of the electron beam and since the tug potential keeps increasing, the debris potential has to decrease. The potential difference between the tug and debris (third from top of Fig. 7) keeps increasing with increasing beam electron current. The bottom figure shows the product of the tug and Debris potentials, which is a proxy for the electrostatic attractive force. The vertical line indicates the $\phi_T = -\phi_D$ conditions, i.e. where the absolute values of the tug and the debris potentials are equal. As seen, this is not the location of the maximum electrostatic force. In this scenario, the maximum electrostatic tractor force is around the $\phi_T = U/2$ potential, but the debris has a smaller potential magnitude. The force is a flat function of the active beam emission current and thus the tug–debris interaction is insensitive to small potential variations that could be caused by varying plasma conditions, for example.

6. Conclusions and summary

It is tempting to have as small separation as safely possible without the risk of collision. However, it is important to keep in mind that the electrostatic force magnitude can vary significantly as the towed vehicle's orientation changes. In particular, the more non-spherical the second vehicle is, the larger these force variations can be. A cause of this is the induction charge redistribution. Thus, to fly less than 1 craft radii apart, it is important to have a detailed model and knowledge of the debris geometry. However, with a robust stationkeeping feedback control method, these force variations have been shown to have a minor variation on the ET efficiency for debris mitigation. Another reason for being cautious of flying too close is the recapturing of the secondary charge that the debris will emit, such as photoelectrons or secondary electrons. Future analysis will explore an optimal distance for operation which considers such recapture events.

To increase the electrostatic tractor (ET) effectiveness, the tug should be made roughly at least the size of the debris to be moved. The larger vehicle radius provides the benefit of a larger capacitance, and thus larger electrostatic force at the same potential. Note that a large tug dimension does not mean necessarily a large tug mass. Rather, a lightweight charged outer tug surface is envisioned to provided the desired capacitance. The equal potential condition between tug and debris is shown to provide the largest electrostatic tractor performance if the two bodies have a similar size, or the separation distance is comparatively large.

Finally, the numerical simulations including plasma conditions illustrate that non-idealized maximum ET potential are close to the equal potential solution. The insight that the maximum ET force is insensitive to the precise electron beam current is promising in that it will simplify the ET sensing and control concerns.

Acknowledgment

Thanks to Dr. Daniel F. Moorer and the Wacari Group for their support of this work, and DARPA who sponsored the electrostatic space debris removal SBIR Phase I study. Thanks also goes to Erik Hogan to helped with the numerical simulation validation and illustration.

References

Anderson, Paul V., Schaub, Hanspeter, 2013. Local orbital debris flux study in the geostationary ring. Adv. Space Res. 51 (12), 2195–2206. http://dx.doi.org/10.1016/j.asr.2013.01.019 http://www.sciencedirect.com/science/article/pii/S0273117713000410.

Bombardelli, Claudio, Pelaez, Jesus, 2011. Ion beam shepherd for contactless space debris removal. AIAA J. Guid. Control Dyn. 34 (3), 916–920. http://dx.doi.org/10.2514/1.51832.

Bombardelli, Claudio, Urrutxua, Hodei, Merino, Mario, Ahedo, Eduardo, Pelaez, Jesus, Olympio, Joris, 2011. Dynamics of ion-beam propelled space debris. In: International Symposium on Space Flight Dynamics, Sao Jose dos Campos, Brasil, February 28–March 4, 2011.

Bosse, Albert B., James Barnds, W., Brown, Michael A., Glenn Creamer, N., Feerst, Andy, Glen Henshaw, C., Hope, Alan S., Kelm, Bernard E., Klein, Patricia A., Pipitone, Frank, Plourde, Bertrand E., Whalen, Brian P., 2004. Sumo: spacecraft for the universal modification of orbits. International Society for Optical Engineering, vol. 5419. SPIE, pp. 36–46.

Castronuovo, Marco M., 2011. Active space debris removal – a preliminary mission analysis and design. Acta Astronaut. 69, 848–859.

Chrystal, Philip, McKnight, Darren, Meredith, Pamela L., Schmidt, Jan, Fok, Marcel, Wetton, Charles, 2011. Space debris: on collision course for insurers? Technical report, Swiss Reinsurance Company Ltd, Zürich, Switzerland.

Cover, John H., Knauer, Wolfgang, Maurer, Hans A., 1966. Lightweight reflecting structures utilizing electrostatic inflation. US Patent 3,546,706.

Denton, M.H., Thomsen, M.F., Korth, H., Lynch, S., Zhang, J.C., Liemohn, M.W., 2005. Bulk plasma properties at geosynchronous orbit. J. Geophys. Res. 110 (A7). http://dx.doi.org/10.1029/2004JA010861.

Draine, B.T., Salpeter, E.E., 1979. On the physics of dust grains in hot gas. Astrophys. J. 231, 77–94. http://dx.doi.org/10.1086/157165.

Hogan, Erik, Schaub, Hanspeter, 2012. Space debris reorbiting using electrostatic actuation. In: AAS Guidance and Control Conference, Breckenridge CO., February 3–8, 2012. Paper AAS 12-016.

Hogan, Erik, Schaub, Hanspeter, 2013. Relative motion control for two-spacecraft electrostatic orbit corrections. AIAA J. Guid. Control Dyn. 36 (1), 240–249.

Janhunen, P., Envall, J., Kvell, U., Noorma, M., Seppanen, H., Haeggstrom, E., Praks, J., Kalvas, T., Koivisto, H., Obratszov, A., Rosta, R., 2013. Cubesat measurement and demonstration of coulomb drag effect for deorbiting. In: Sixth European Conference on Space Debris, Darmstadt, Germany, April 22–25, 2013.

Jasper, Lee E.Z, Schaub, Hanspeter, 2012. Effective sphere modeling for electrostatic forces on a three-dimensional spacecraft shape. In: Alfriend, Kyle T., Akella, Maruthi, Hurtado, John E., Juang, Jer-Nan, Turner, James D. (Eds.), Adventures on the Interface of Dynamics and Control. Tech Science Press, Duluth, Georgia, pp. 267–298.

Jehn, Rüdiger, Agapov, V., Hernández, Cristina, 2005. The situation in the geostationary ring. Adv. Space Res. 35 (7), 1318–1327.

Johnson, Nicholas L., 2010. Orbital debris: the growing threat to space operations. In: 33rd Annual AAS Guidance and Control Conference, Breckenridge CO., February 6–10, 2010. Paper AAS 10-011.

Kawamoto, Satomi, Makida, Takeshi, Sasaki, Fumiki, Okawa, Yasushi, Nishida, Shinichiro, 2006. Precise numerical simulations of electrody-

namic tethers for an active debris removal system. Acta Astronaut. 59 (1–5), 139–148. http://dx.doi.org/10.1016/j.actaastro.2006.02.035 http://www.sciencedirect.com/science/article/pii/S0094576506000968.

King, Lyon B., Parker, Gordon G., Deshmukh, Satwik, Chong, Jer-Hong, 2003. Study of interspacecraft coulomb forces and implications for formation flying. AIAA J. Propul. Power 19 (3), 497–505.

Kitamura, S., 2010. Large space debris reorbiter using ion beam irradiation. In: 61st International Astronautical Congress, Prague, Czech Republic, September 27–October 1, 2010.

Korth, H., Thomsen, M.F., Borovsky, J.E., McComas, D.J., 1999. Plasma sheet access to geosynchronous orbit. J. Geophys. Res. 104 (A11), 25047–25062. http://dx.doi.org/10.1029/1999JA900292 http://ads-abs.harvard.edu/abs/1999JGR10425047K.

Lai, Shu T, 2011. Fundamentals of Spacecraft Charging: Spacecraft Interactions with Space Plasmas. Princeton University Press.

Liou, J.-C., 2011. Active debris removal – a grand engineering challenge for the twenty-first century. In: AAS Spaceflight Mechanics Meeting, New Orleans, LA, February 13–17, 2011. Paper AAS 11-254.

Moorer, Daniel F., Schaub, Hanspeter, 2011a. Electrostatic spacecraft reorbiter. US Patent 8,205,838 B2.

Moorer, Daniel F., Schaub, Hanspeter, 2011b. Hybrid electrostatic space tug. US Patent 0036951-A1.

Mullen, E.G., Gussenhoven, M.S., Hardy, D.A., Aggson, T.A., Ledley, B.G., 1986. Scatha survey of high-voltage spacecraft charging in sunlight. J. Geophys. Res. 91 (A2), 1474–1490. http://dx.doi.org/10.1029/JA091iA02p01474.

Murdoch, Naomi, Izzo, Dario, Bombardelli, Claudio, Carnelli, Ian, Hilgers, Alain, Rodgers, David, 2008. The electrostatic tractor for asteroid deflection. In: 58th International Astronautical Congress. Paper IAC-08-A3.I.5.

Natarajan, Arun, Schaub, Hanspeter, 2008. Orbit-nadir aligned coulomb tether reconfiguration analysis. J. Astronaut. Sci. 56 (4), 573–592.

Pearson, Jerome, Carroll, Joseph, Levin, Eugene, Oldson, John, Hausgen, Paul, 2003. Overview of the electrodynamic delivery express (edde). In: 39th AIAA/ASME/SAE/ASEE Joint Propulsion Conference and Exhibit, Huntsville, AL, July 20–23, 2003. AIAA-2003-4790.

Peck, Mason A., 2005. Prospects and challenges for lorentz-augmented orbits. In: AIAA Guidance, Navigation and Control Conference, San Francisco, CA, August 15–18, 2005. Paper No. AIAA 2005-5995.

Pfau, S., Tichy, M., 2001. Low Temperature Plasma Physics: Fundamental Aspects and Applications. Wiley, Berlin.

Richards, Matthew G., Springmann, Philip N., McVey, Michelle E., 2005. Assessing the challenges to a geosynchronous space tug system. In: Modeling, Simulation, and Verification of Space-based Systems II, vol. 5799, pp 135–145.

Schaub, Hanspeter, Jasper, Lee E.Z., 2011. Circular orbit radius control using electrostatic actuation for 2-craft configurations. In: AAS/AIAA Astrodynamics Specialist Conference, Girdwood, Alaska, July 31–August 4, 2011. Paper AAS 11-498.

Schaub, Hanspeter, Jasper, Lee E.Z., 2013. Orbit boosting maneuvers for two-craft coulomb formations. AIAA J. Guid. Control Dyn. 36 (1), 74–82.

Schaub, Hanspeter, Moorer, Daniel F., 2010. Geosynchronous large debris reorbiter: challenges and prospects. In: AAS Kyle T. Alfriend Astrodynamics Symposium, Monterey, CA, May 17–19, 2010. Paper No. AAS 10-311.

Sliško, Josip, Brito-Orta, Raúl A., 1998. On approximate formulas for the electrostatic force between two conducting spheres. Am. J. Phys. 66 (4), 352–355.

Smith, D.A., Martin, C., Kassebom, M., Petersen, H., Shaw, A., Skidmore, B., Smith, D., Stokes, H., Willig, A., 2004. A mission to preserve the geostationary region. Adv. Space Res. 34 (5), 1214–1218. http://dx.doi.org/10.1016/j.asr.2003.02.042, ISSN 0273–1177 http://www.sciencedirect.com/science/article/B6V3S-4C2NJ48-2/2/45303240a46d3cdb9b44a584608adfe0.

Soules, Jack A., 1990. Precise calculation of the electrostatic force between charged spheres including induction effects. Am. J. Phys. 58, 1195–1199.

Sternovsky, Zoltán, Němeček, Zdeněk, Šafránková, Jana, Velyhan, Andriy, 2001. Ion field emission from micrometer-sized spherical glass grains. IEEE Trans. Plasma Sci. 29 (2), 292–297.

Sternovsky, Zoltán, Chamberlin, P., Horanyi, M., Robertson, S., Wang, X., 2008. Variability of the lunar photoelectron sheath and dust mobility due to solar activity. J. Geophys. Res.: Space Phys. 113 (A10). http://dx.doi.org/10.1029/2008JA013487.

Stiles, Laura A., Seubert, Carl R., Schaub, Hanspeter, 2012. Effective coulomb force modeling in a space environment. In: AAS Spaceflight Mechanics Meeting, Charleston, South Carolina, January 29–February 2, 2012. Paper AAS 12.

Wang, Shuquan, Schaub, Hanspeter, 2011. Nonlinear charge control for a collinear fixed shape three-craft equilibrium. AIAA J. Guid. Control Dyn. 34 (2), 359–366. http://dx.doi.org/10.2514/1.52117.

Xu, Wenfu, Liang, Bin, Li, Bing, Xu, Yangsheng, 2011. A universal on-orbit servicing system used in the geostationary orbit. Adv. Space Res. 48 (1), 95–119. http://dx.doi.org/10.1016/j.asr.2011.02.012 http://www.sciencedirect.com/science/article/pii/S0273117711001402.

Žilavý, P., Sternovsky, Zoltán, Čermak, I., Němeček, Zdeněk, Šafránková, Jana, 1998. Surface potential of small particles charged by the medium-energy electron beam. Vacuum 50 (1–2), 139–142.